Self-consistent field theory of adsorption of flexible polyelectrolytes onto an oppositely charged sphere*

Tong Zhao-Yang(童朝阳)[a], Zhu Yue-Jin(诸跃进)[b], and Tong Chao-Hui(童朝晖)[b]†

[a] Department of Physics, Hunan Normal University, Changsha 415001, China
[b] Department of Physics, Ningbo University, Ningbo 315211, China

(Received 10 June 2013; revised manuscript received 3 September 2013; published online 24 January 2014)

The adsorption of flexible polyelectrolyte (PE) with the smeared charge distribution onto an oppositely charged sphere immersed in a PE solution is studied numerically with the continuum self-consistent field theory. The power law scaling relationships between the boundary layer thickness and the surface charge density and the charge fraction of PE chains revealed in the study are in good agreement with the existing analytical result. The curvature effect on the degree of charge compensation of the total amount of charges on the adsorbed PE chains over the surface charges is examined, and a clear understanding of it based on the dependences of the degree of charge compensation on the surface charge density and the charge fraction of PE chains is established.

Keywords: polyelectrolyte, adsorption, self-consistent field theory

PACS: 82.35.Rs, 68.47.Pe, 41.20.Cv **DOI:** 10.1088/1674-1056/23/3/038202

1. Introduction

Polyelectrolytes (PEs) are polymers with ionizable functional groups on the polymer chain backbones. PEs are interesting from a theoretical point of view and have a wide range of technical applications, and are also of crucial importance in the perspective of biological and life sciences.[1–10] There are many interesting phenomena related to PEs, some of which may appear counter-intuitive, such as the like-charge attraction mediated by PEs. The adsorption of PEs on oppositely charged objects has drawn great attention in recent decades.[11–32] In the absence of the short range PE-surface non-electrostatic interaction, the PE adsorption is mainly governed by the competition between the PE-surface attractive electrostatic interaction and the entropy loss of the polymer chains upon the adsorption. The understanding of the PE adsorption lags behind that of the neutral polymer adsorption because the PE adsorption is much more complicated due to the long-range nature of the Coulomb electrostatic interaction and the additional length scales introduced by PEs and the mobile ions.

A central aspect of PE adsorption is the so-called charge inversion, that is, the total amount of charges on adsorbed PE chains overcompensates that of the surface charges of the object.[13–17,21–23] Other interesting issues regarding the PE adsorption, such as the thickness of the polymer layer, the critical condition for the adsorption, the effect of the added salt ions, the effect of short-range PE-surface non-electrostatic interaction, the influence the smeared (corresponding to strongly dissociating PEs) and annealed (corresponding to weakly dissociating PEs) charge distributions, and the difference between planar and curved (cylindrical, spherical) charged objects, have also attracted the research attention.[13–23]

In the study of PE adsorption, molecular simulation methods such as molecular dynamics (MD), Monte Carlo (MC), and Brownian dynamics (BD), are extensively used.[24–26,33–35] They have the advantage of accurately computing the Coulomb electrostatic interaction. On the other hand, coarse-grained numerical methods such as the self-consistent field theory (SCFT) have also been employed to study the PE adsorption.[13–17,21–23] They are computationally cheap and provide an attractive alternative to the study of polyelectrolytes. The continuum SCFT have been applied to the study of the adsorption of PEs on charged planar and cylindrical surfaces.[13,14] Recently, the continuum SCFT was adopted to numerically study the adsorption of PEs with the smeared charge distribution on an oppositely charged sphere in the ground dominance limit.[15] The effects of the added salt ions and the short-range PE-surface non-electrostatic interaction were investigated in the study. In our previous works, the continuum SCFT for flexible PEs was employed to study the adsorption of PEs with the smeared charge distribution onto two oppositely charged columns with a square cross-section,[21,22] and the curvature effect of a charged curved surface was not considered. In this work, we apply the continuum SCFT for PEs to the study of the adsorption of PEs with the smeared charge distribution onto an oppositely charged sphere

*Project supports by the National Natural Science Foundation of China (Grant Nos. 21074062 and 11174163), the Scientific Research Foundation for the Returned Overseas Chinese Scholars, Ministry of Education of China, and the Scientific Research Fund of Zhejiang Provincial Educational Department, China (Grant No. Y200907455).

†Corresponding author. E-mail: tongchaohui@nbu.edu.cn

© 2014 Chinese Physical Society and IOP Publishing Ltd

immersed in a PE solution. The curvature effect of the charged sphere on the degree of charge compensation is carefully examined. The rest of the paper is organized as follows. In Section 2, the theory and SCF equations for PEs with the smeared charge distribution are described. In Section 3, results and discussion regarding the boundary layer scaling, the degree of charge compensation, and the curvature effect of the charged sphere are presented. In Section 3, the main results are summarized.

2. Theory and model equations

In this work, we consider a flexible PE solution with the smeared charge distribution in which a spherical object with uniform surface charges of the opposite sign is immersed and study the adsorption of PE chains onto the charged sphere. For numerical convenience, the PE solution is confined in a much bigger concentric sphere of radius R_s than the charged sphere of radius R and the bigger sphere has a neutral hard wall, and then the system size is $V = 4\pi\left(R_s^3 - R^3\right)/3$. It will be shown later in the paper that the spherical geometry of the system under study and the hard wall exerts no influence on the adsorption behaviors of PE chains onto an oppositely charged sphere as long as the system size, i.e., the radius of the sphere in which the PE solution is confined, is large enough.

The continuum SCFT theory for an inhomogeneous multi-component weakly charged polyelectrolyte system has been derived in Refs. [27] and [28]. The dimensionless SCF equations are as follows:

$$\phi_{\rm P}(\boldsymbol{r}) + \phi_{\rm S}(\boldsymbol{r}) - 1 = 0, \tag{1}$$

$$\omega_{\rm P}(\boldsymbol{r}) = \chi_{\rm PS} N \phi_{\rm S}(\boldsymbol{r}) + \eta(\boldsymbol{r}), \tag{2}$$

$$\omega_{\rm S}(\boldsymbol{r}) = \chi_{\rm PS} N \phi_{\rm P}(\boldsymbol{r}) + \eta(\boldsymbol{r}), \tag{3}$$

$$\omega_{\pm} = N\nu_{\pm}\psi(\boldsymbol{r}), \tag{4}$$

$$\phi_{\rm P}(\boldsymbol{r}) = \frac{\bar{\phi}_{\rm P}}{Q_{\rm P}} \int_0^1 {\rm d}s q(\boldsymbol{r},s) q(\boldsymbol{r},1-s), \tag{5}$$

$$\phi_M(\boldsymbol{r}) = \frac{\bar{\phi}_M}{Q_M} \exp\left[-\frac{\omega_M(\boldsymbol{r})}{N}\right], \tag{6}$$

$$\nabla\cdot[\varepsilon(\boldsymbol{r})\nabla\psi(\boldsymbol{r})] = -N\left[\alpha_{\rm P}\nu_{\rm P}\phi_{\rm P}(\boldsymbol{r}) + \nu_+\phi_+(\boldsymbol{r}) + \nu_-\phi_-(\boldsymbol{r})\right]. \tag{7}$$

In the above equations, ϕ_j with $j = {\rm P}$, S, and $\pm$ are the dimensionless volume fractions of PE chains, solvent molecules, and mobile ions, the incompressibility of the system is enforced through the introduction of the Lagrange multiplier $\eta(\boldsymbol{r})$ (see Eqs. (2) and (3)), $\chi_{\rm PS}$ denotes the Flory–Huggins interaction parameter between monomers and solvent molecules, ω_j denotes the conjugate interaction field within the SCFT formalism, $\psi(\boldsymbol{r})$ denotes the electric potential field, the volume-averaged densities $\bar{\phi}_{\rm P} \equiv n_{\rm P}N/(\rho_0 V)$ and $\bar{\phi}_M \equiv n_M/(\rho_0 V)$ with $n_{\rm P}$ and n_M representing respectively the total number of PE chains with a chain length N and species M ($M = {\rm S}, +, -$), ρ_0 denotes the same density of PE segments and the solvent molecules, $\varepsilon(\boldsymbol{r})$ denotes the permittivity, $Q_{\rm P} = \int {\rm d}\boldsymbol{r} q(\boldsymbol{r},1)/V$, $Q_M = \int {\rm d}\boldsymbol{r}\exp[-\omega_M/N]/V$. In the present study, the permittivity of the medium is assumed to be a constant, the same as that of the pure water. In Eq. (7), $\alpha_{\rm P}$ denotes the average degree of ionization or the charge fraction of PE chains with the smeared charge distribution, $\nu_{\rm P} = -1$, $\nu_\pm = \pm 1$ are for the charge valences of PE chains and the mobile ions respectively. In this relatively short paper, we limit our attention to a salt-free PE solution, and the effect of short-range PE-surface non-electrostatic interaction will not be considered. Thus, $\phi_+(\boldsymbol{r})$ refers to the dimensionless number density of counter-ions which come from the ionization of the functional groups on PE chains, whereas $\phi_-(\boldsymbol{r})$ denotes the dimensionless number density of co-ions which come from the ionization of the functional groups on the sphere and the sphere is then positively charged. Moreover, because the number densities of counter-ions and co-ions in this study are rather low, which are on the order of 10^{-4}–10^{-3}, the effect of size of these mobile ions is not considered (see Eq. (1)).

The propagator $q(\boldsymbol{r},s)$ corresponding to the probability of finding the end-segment of a polymer chain of length s at $\boldsymbol{r}$ satisfies the following modified diffusion equation

$$\frac{\partial q(\boldsymbol{r},s)}{\partial s} = \nabla^2 q(\boldsymbol{r},s) - \omega_{\rm p}(\boldsymbol{r}) q(\boldsymbol{r},s). \tag{8}$$

To study the charge inversion phenomenon, the parameter of the degree of charge compensation is introduced as follows:

$$\Xi = \int_V \alpha_{\rm p}\left[\phi_{\rm p}(\boldsymbol{r}) - \phi_{\rm f}(\boldsymbol{r})\right] {\rm d}^3\boldsymbol{r}/Q, \tag{9}$$

where Q is the total amount of charges on the surface of the charged sphere, $\phi_{\rm f}(\boldsymbol{r})$ denotes the volume fraction of the free chains in the system. To study the PE adsorption on the charged sphere and calculate different chain conformations, the region between the surface of the sphere and the second inflection point of the monomer radial density profile away from the charged sphere is defined as the boundary layer. The free chains that are not adsorbed onto the charged sphere are calculated as $\phi_{\rm f}(\boldsymbol{r}) = \left(\bar{\phi}_{\rm P}/Q_{\rm P}\right)\int_0^1 {\rm d}s q^{\rm f}(\boldsymbol{r},s) q^{\rm f}(\boldsymbol{r},1-s)$. The propagator $q^{\rm f}(\boldsymbol{r},s)$ corresponds to PE chains with none of their segments falling into the boundary layer. Please refer to Ref. [21] for the calculations of the adsorbed PE chains with tail, loop and train conformations.

To elucidate the relations between the distributions of counter-ions and co-ions and the surface charge density of the sphere, the relative amount of the total charges of the counter-ions and co-ions inside the boundary layer are computed as follows:

$$\Xi_+ = \int_{\rm BL} \phi_+(\boldsymbol{r}) {\rm d}^3\boldsymbol{r}/Q, \tag{10}$$

$$\Xi_- = \int_{\rm BL} \phi_-(\boldsymbol{r}) {\rm d}^3\boldsymbol{r}/Q, \tag{11}$$

where BL denotes the volume occupied by the boundary layer.

To numerically solve the SCF equations, it is natural to use a spherical coordinate system (r,θ,ϕ) where the center of the sphere is placed at the origin. Furthermore, it is quite reasonable to assume that all the physical quantities have no dependence on the two angular coordinates θ, ϕ, and vary only along the radial direction. Thus, the dimensionality of the problem is reduced to one. Accordingly, the volume element is transformed to $\mathrm{d}V \equiv \mathrm{d}^3\boldsymbol{r} = 4\pi r^2 \mathrm{d}r$.

In numerically solving the SCF equations, the grid size of the one-dimensional computational domain is set to $0.03125R_\mathrm{g}$ or $0.015625R_\mathrm{g}$ (R_g is the radius of gyration of a flexible PE chain), and the time step size for solving $q(r,s)$ is 0.01. The modified diffusion equation and the Poisson equation are solved by using the standard linear multigrid method.[21] On the surface of the charged sphere, the Neumann boundary condition of $(\partial\psi/\partial r)|_\mathrm{BC} = (6N)^{1/2}\sigma b^2/\varepsilon$ in the dimensionless form is applied,[21] and $q = 0$. On the hard wall of the spherical system, that is at $r = R_\mathrm{s}$, $q = 0$, $\partial\psi/\partial r = 0$. Furthermore, the zero reference electric potential is located at $r = R_\mathrm{s}$.

3. Results and discussion

In this paper, for simplicity, the segment size is set as $b = 0.7$ nm, the chain length of PE chain is fixed as $N = 50$, the Flory–Huggins parameter $\chi_\mathrm{PS} = 0.0$. The bulk monomer volume fraction is fixed as 0.005, which is not far from the chain overlapping concentration ϕ^* for a semi-dilute polymer solution with $\phi^* = Nb^3/\left(N^{3/5}b\right)^3 \approx 0.04$. The radius of the charged sphere is varied from 0.75 to $10.0R_\mathrm{g}$. The dimensionless dielectric constant of the system is fixed at $\varepsilon = 0.4762$, which corresponds to the dielectric constant of pure water at room temperature. The charge fraction of a PE chain is varied from $\alpha_\mathrm{p} = 0.05$ to $\alpha_\mathrm{p} = 0.3$. Note that the range of α_p can be estimated by equating the electrostatic energy of a charged polymer coil in a good solvent to the thermal energy, i.e.,

$$\frac{\left(N\alpha_\mathrm{p}\right)^2 e^2}{\varepsilon_0\varepsilon_\mathrm{r}\left(N^{3/5}b\right)} \sim k_\mathrm{B}T \Rightarrow \alpha_\mathrm{p} \sim N^{-7/10} l_\mathrm{B}^{-1/2} b^{1/2}, \qquad (12)$$

where $l_\mathrm{B} = e^2/(\varepsilon_0\varepsilon_\mathrm{r}k_\mathrm{B}T)$ is the Bjerrum length which is about 0.7 nm in water at room temperature (ε_0, ε_r denote the vacuum permittivity and the dielectric constant respectively). For a PE chain length $N = 50$, $\alpha_\mathrm{p} \sim 0.065$. The sphere is positively charged with a surface charge density of σ. The product of σ and b^2 is varied from $\sigma b^2 = 0.02381$ to $\sigma b^2 = 0.19048$, which corresponds to a charge density of $\sigma = 4.857 \times 10^{-2}$ nm^{-2} to $\sigma = 3.8856 \times 10^{-1}$ nm^{-2}.

3.1. Scaling relationships between the boundary layer thickness and the surface charge density of the spherical particle/the charge fraction of PE chains

It can be clearly seen from Fig. 1 and its inset that, for the PE adsorption on an oppositely charged sphere, the boundary layer thickness scales with both the surface charge density and the charge fraction of PE chains as a power law. The scaling exponent is -0.35 for both scaling relationships. This scaling exponent is in good agreement with the analytical result obtained from the Green's function equation in the ground state dominance limit. For PE chains with a smeared charge distribution, the Green's function method suggests that the surface charge density and the charge fraction of PE chains form a universal parameter governing the boundary layer thickness, and the scaling exponent remains as $-1/3$ for both planar and curved (cylindrical and spherical) charged surfaces.[18–20]

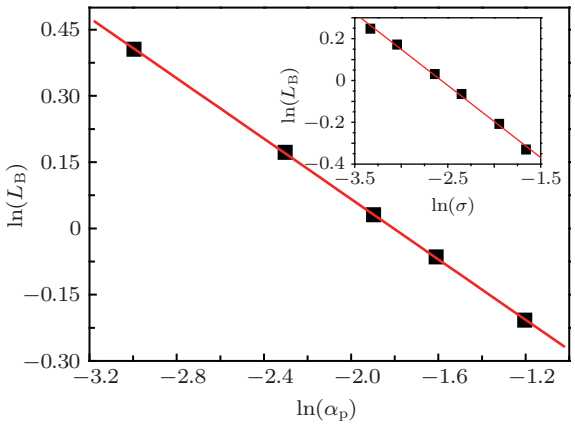


Fig. 1. (color online) The double logarithmic plot of the boundary layer thickness against the charge fraction of PE chains for a sphere with $R = 1.0R_\mathrm{g}$ at a surface charge density of $\sigma b^2 = 0.09524$. In the inset, the double logarithmic plot of the boundary layer thickness against the surface charge density at a PE monomer charge fraction of $\alpha_\mathrm{p} = 0.2$ for a sphere with $R = 1.0R_\mathrm{g}$ is displayed.

The effects of the radius of the charged sphere on the boundary layer thickness L_B and the scaling laws between L_B and α_p, σ are investigated. It is found from the numerical study that L_B decreases slightly with the increase of the radius and L_B eventually reaches a constant for the radius larger than about $5.0R_\mathrm{g}$ (see the inset of Fig. 2), thus approaching the planar surface limit. Our numerical study shown in Fig. 3 reveals that, in the planar surface limit, the scaling exponents between L_B and α_p, σ are both -0.33, which is in excellent agreement with the analytical result from the Green's function method.[18–20] It should also be noted that, the scaling exponent of -0.33 is also in good agreement with our numerical result of the PE adsorption on two charged columns with a square cross-section.[21,22] It should be pointed out that the scaling laws obtained here only apply to the scenario in which the PE chains are weakly charged and flexible, and the adsorption substrate is also weakly charged. A weakly charged surface can be quantitatively defined by the electrostatic coupling

constant proposed by Netz *et al.*,[31] which is equal to $4\pi l_B^2\sigma$. A weakly charged surface corresponds to an electrostatic coupling constant ≤ 1 under which the mean-field theories such as SCFT work well. The highest surface charge density of 0.19048 studied in this paper corresponds to an electrostatic coupling constant of about 2.4, which is not far away from this limit. Furthermore, it should be noted that the advantage of SCFT over the Green's function method is that the different chain conformations can be quantified. The Green's function method is unable to calculate the total amount of the adsorbed chains or the degree of charge compensation.

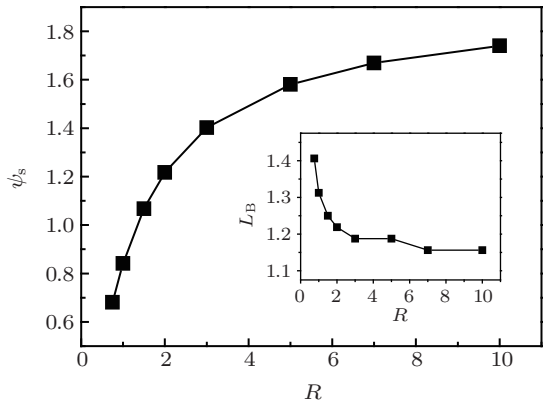


Fig. 2. The magnitude of the dimensionless particle surface electric potential is plotted against the radius of the charged sphere at $\alpha_p = 0.2$, $\sigma = 0.04762$. The radius of the sphere is in the unit of R_g. In the inset, the boundary layer thickness is plotted against the radius of the charged sphere at $\alpha_p = 0.2$, $\sigma = 0.04762$.

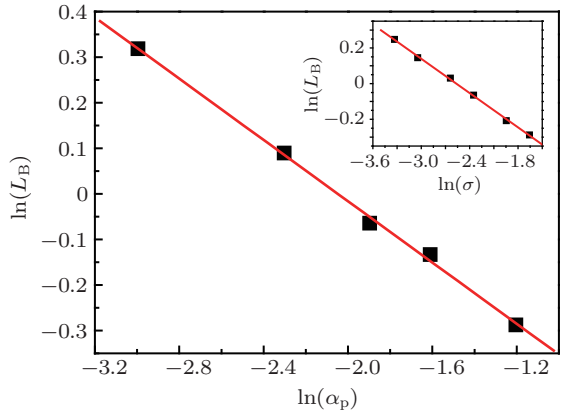


Fig. 3. (color online) The double logarithmic plot of the boundary layer thickness against the charge fraction of PE chains for a sphere with $R = 6.0R_g$ at a surface charge density of $\sigma b^2 = 0.09524$. In the inset, the double logarithmic plot of the boundary layer thickness against the surface charge density at a PE monomer charge fraction of $\alpha_p = 0.15$ for a sphere with $R = 6.0R_g$ is shown. The slopes in the figure and the inset are -0.33.

The trend of the boundary layer thickness with the variation of the radius of the charged sphere is likely due to the influence of the surface electric potential. Imagine that an isolated and uniformly charged sphere is imbedded in an infinitely large dielectric medium, it is straightforward to show that the surface electric potential is $\psi_s = \sigma R/\varepsilon_0\varepsilon_r$. Thus, the surface potential linearly increases with the radius. In the present study, the surface electric potential can be obtained by numerically solving the Poisson equation (i.e., Eq. (7)). A typical example of the variation of the surface potential with the sphere radius is shown in Fig. 2. Evidently, the magnitude of the surface potential increases with the radius of the charged sphere, and levels off in the large radius limit.

3.2. Effects of the system size on the boundary layer thickness and the degree of charge compensation of PE chains adsorbed on an oppositely charged sphere

For the PE adsorption onto an oppositely charged sphere studied in this paper, we employ a spherical system capped by a hard wall in which there is a PE solution and a spherical oppositely charged sphere, and the spherical system and the charged sphere are concentric. The adoption of such a spherical system capped by a hard wall is for the sake of the numerical convenience. As long as the radius of the spherical system is large enough compared with the radius of the charged sphere, the effect of confinement of the hard wall on the adsorption behaviors of PEs can be removed. As can be clearly seen from Fig. 4 and the inset, for a large enough system size, the effect of confinement of the hard wall indeed exerts no influence on the boundary layer thickness and the degree of charge compensation.

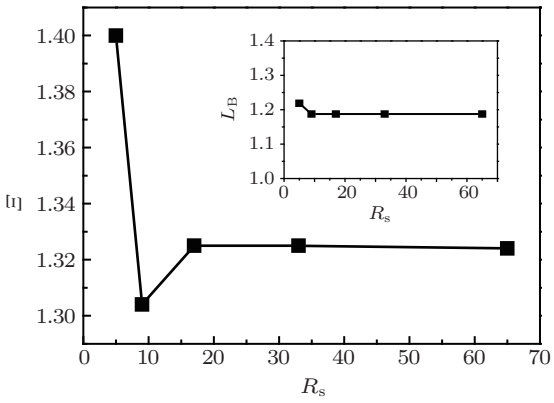


Fig. 4. The plot of the degree of charge compensation against the radius of the spherical system at $\sigma b^2 = 0.04762$ and $\alpha_p = 0.2$. In the inset, the boundary layer thickness is plotted against the radius of the spherical system at $\sigma b^2 = 0.04762$ and $\alpha_p = 0.2$.

3.3. Dependence of the degree of charge compensation of PE chains adsorbed on an oppositely charged sphere on the charge fraction of PE chains and the surface charge density

Our numerical results suggest that, for the PE adsorption on an oppositely charged sphere and in the absence of short-range non-electrostatic PE-surface interactions, the degree of charge compensation of the total amount of charges on the adsorbed chains over the surface charges increases with increasing charge fraction of PE chains (see Fig. 5), but decreases

with the increase of the surface charge density (see the upper left inset of Fig. 5). Such trends are identical to those for the PE adsorption on two oppositely charged columns with square cross-section in our previous study.[21] Please note that the absolute amount of the adsorbed PE chains increases with the surface charge density (see the lower right inset of Fig. 5).

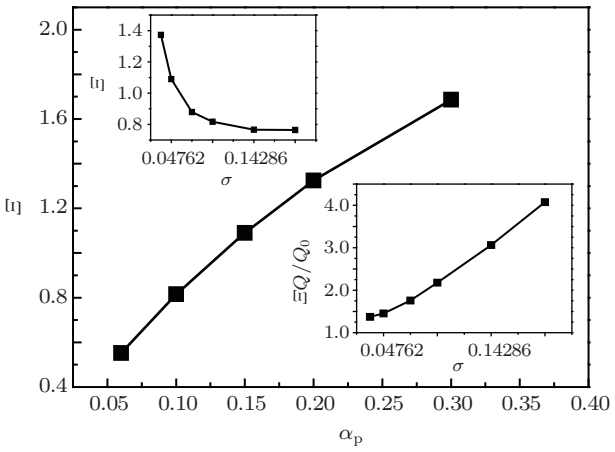


Fig. 5. The plot of the degree of charge compensation against the charge fraction of PE chains at a surface charge density of $\sigma b^2 = 0.04762$ and $R = 1.0R_g$. In the upper left inset, the plot of the degree of charge compensation against the surface charge density at a PE charge fraction of $\alpha_p = 0.15$ and $R = 1.0R_g$ is displayed. In the lower right inset, the plot of the total amount of charges on the adsorbed PE chains against the surface charge density is displayed with the same system parameters as in the upper left inset. In the label of the y axis in the lower right inset, Q denotes the total surface charges on the sphere, Q_0 denotes the total surface charges at $\sigma b^2 = 0.03572$, which is used to normalize the total amount of charges on the adsorbed chains.

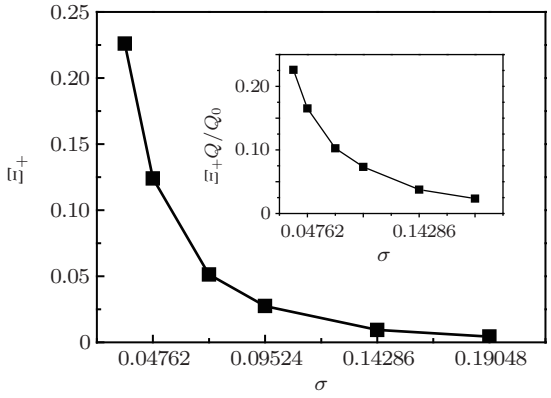


Fig. 6. The plot of the relative amount of charges of counter-ions inside the boundary layer against the surface charge density at the same system parameters as in Fig 5. In the inset, the plot of the total amount of charges of the counter-ions inside the boundary layer against the surface charge density is displayed with the same system parameters as in the figure. In the label of the y axis in the inset, Q denotes the total surface charges on the sphere, Q_0 denotes the total surface charges at $\sigma b^2 = 0.03572$.

Another interesting aspect of PE adsorption on the charged sphere is the relations between the distributions of the mobile ions and the surface charge density.[30,32] As shown in Fig. 6 and its inset, the relative and absolute amounts of the positive counter-ions inside the boundary layer decrease with the increase of the surface charge density. This is because both the counter-ions and the surface charges on the sphere are of the same charge sign. For negatively charged co-ions, with the increase of the surface charge density of the sphere, due to the stronger electrostatic attraction between the co-ions and the surface charges, the absolute amount of the co-ions inside the boundary layer also increases as shown in the inset of Fig. 7. On the other hand, the relative amount of the co-ions inside the boundary layer shows a nontrivial dependence on the surface charge density, as revealed from Fig. 7.

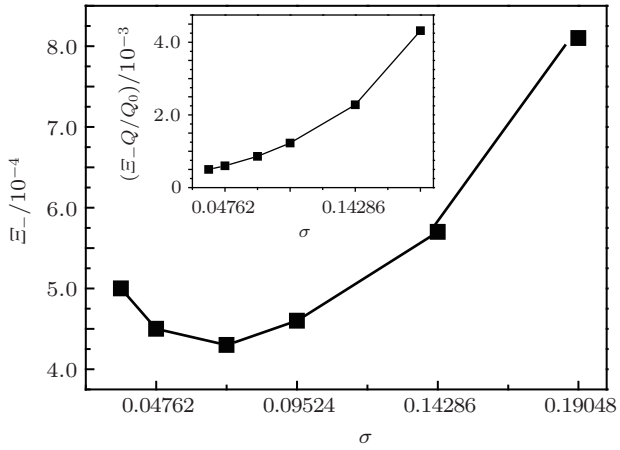


Fig. 7. The plot of the relative amount of charges of co-ions inside the boundary layer against the surface charge density at the same system parameters as in Fig. 5. In the inset, the plot of the total amount of charges of the co-ions inside the boundary layer against the surface charge density is displayed with the same system parameters as in the figure. In the label of the y axis in the inset, Q denotes the total surface charges on the sphere, Q_0 denotes the total surface charges at $\sigma b^2 = 0.03572$.

3.4. Effect of the radius of charged sphere on the degree of charge compensation of PE chains adsorbed on an oppositely charged sphere

It can be clearly seen from Fig. 8 that the degree of charge compensation of the adsorbed PE chains Ξ shows interesting and unusual dependence on the radius of the charge sphere. At relatively low surface charge density σ and high charge fraction α_p, Ξ decreases with the increase of the radius, and eventually saturates in the planar surface limit. On the other hand, at relatively high surface charge density σ and low α_p, Ξ increases with the increase of the radius, and levels off for large enough radius. The numerical study in subsection *C* clearly suggests that Ξ increases with the increase of α_p, but decreases with the increase of σ. Then the different trends of Ξ with varying radius of the charged sphere shown in Fig. 8 can be rationalized as follows. For the parameter combination of relatively low σ and α_p which corresponds to relatively high Ξ, the degree of charge compensation tends to decrease with increasing radius to minimize the electrostatic repulsion between adsorbed PE chains. In the opposite parameter regime which corresponds to relatively low Ξ, Ξ will most likely in-

crease with the increase of the radius before approaching a constant in the planar surface limit.

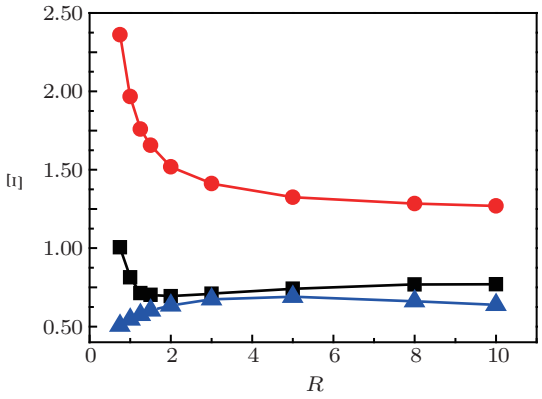


Fig. 8. (color online) The degree of charge compensation of total amount of the charges on the adsorbed PE chains on the surface charges are plotted against the radius of the charged sphere at different surface charge densities and charge fractions of PE chains. In the figure, the curves from the top to the bottom correspond to sets of system parameters of $\sigma = 0.04762$, $\alpha_p = 0.30$; $\sigma = 0.04762$, $\alpha_p = 0.10$; and $\sigma = 0.19048$, $\alpha_p = 0.10$; respectively.

4. Summary

In this paper, the continuum self-consistent field theory is applied to numerically study the adsorption of PEs with the smeared charged distribution onto an oppositely charged sphere immersed in a PE solution. The power law scaling relationships between the boundary layer thickness and the surface charge density and the charge fraction of PE chains are identified in the numerical study. The scaling exponents are in good agreement with the existing analytical result. The surface electric potential likely plays a role in the dependence of the boundary layer thickness on the radius of the charged sphere.

The numerical result reveals interesting trends of the variation of the degree of charge compensation with the radius of the charged sphere. A clear understanding regarding the dependence of the degree of charge compensation on the radius is established. In the parameter regime of low surface charge density and high charge fraction of PE chains, in which the degree of charge compensation is relatively high, the degree of charge compensation decreases with the increase in radius. In the opposite regime which corresponds to relatively low degree of charge compensation, the degree of charge compensation increases with the increase in radius.

Acknowledgment

Tong C H also acknowledges the support from K. C. Wong Magna at Ningbo University, China.

References

[1] Fleer G J, Cohen S M A, Scheutjens J M H M, Gasgove T and Vincent B 1993 *Polymer at Interfaces* (London: Chapman and Hall)
[2] Dautzenberg H, Jaeger W, Kotz J, Philipp B, Seidel C and Stscherbina D 1994 *Polyelectrolytes: Formation, Characterization and Application* (Munich: Hanser Gardner)
[3] Naji A, Seidel C and Netz R R 2006 *Adv. Polym. Sci.* **198** 149
[4] Claesson P M, Dedinaite A and Rojas O 2003 *J. Adv. Colloid Interface Sci.* **104** 53
[5] Dobrynin A V 2008 *Curr. Opin. Colloid Interface Sci.* **13** 376
[6] Podgornik R and Licer M 2006 *Curr. Opin. Colloid Interface Sci.* **11** 273
[7] Ulrich S, Seijo M and Stoll S 2006 *Curr. Opin. Colloid Interface Sci.* **11** 268
[8] Boroudjerdi H, Kim Y W, Naji A, Netz R R, Schlagberger X and Serr A 2005 *Rhys. Rep.* **416** 129
[9] Netz R R and Andelman D 2003 *Phys. Rep.* **380** 1
[10] Claesson P M, Poptoshev E, Blomberg E and Dedinaite A 2005 *Adv. Colloid Interface Sci.* **114** 173
[11] Muthukumar M 1987 *J. Chem. Phys.* **86** 7230
[12] Linse P 1996 *Macromolecules* **29** 326
[13] Man X, Yang S, Yan D D and Shi A C 2008 *Macromolecules* **41** 5451
[14] Wang Q 2005 *Macromolecules* **38** 8911
[15] Wang Z J, Li B H, Ding D T and Wang Q 2011 *Macromolecules* **44** 8607
[16] Messina R, Holm C and Kremer K 2004 *J. Polym. Sci. Part B* **42** 3557
[17] Shafir A, Andelman D and Netz R R 2003 *J. Chem. Phys.* **119** 2355
[18] Winkler R G and Cherstvy A G 2006 *Phys. Rev. Lett.* **96** 066103
[19] Cherstvy A G and Winkler R G 2012 *J. Phys. Chem. B* **116** 9838
[20] Cherstvy A G and Winkler R G 2011 *Phys. Chem. Chem. Phys.* **13** 11686
[21] Tong C, Zhu Y J, Zhang H D, Qiu F, Tang P and Yang Y L 2011 *J. Phys. Chem. B* **115** 11307
[22] Tong C 2012 *J. Chem. Phys.* **137** 104904
[23] Liu Y X, Zhang H D, Tong C and Yang Y L 2011 *Macromolecules* **44** 8261
[24] Netz R R and Joanny J F 1999 *Macromolecules* **32** 9013
[25] Tian W D and Ma Y Q 2010 *Macromolecules* **43** 1575
[26] Ren C L, Tian W D, Szleifer I and Ma Y Q 2011 *Macromolecules* **44** 1719
[27] Shi A C and Noolandi J 1999 *Macromol. Theory Simul.* **8** 214
[28] Wang Q, Taniguchi T and Fredrickson G H 2004 *J. Phys. Chem. B* **108** 6733
[29] Tong C H and Zhu Y J 2010 *Chin. Phys. B* **19** 048702
[30] Lian Z J 2011 *Chin. Phys. Lett.* **28** 058201
[31] Naji A, Jungblut S, Moreira A G and Netz R R 2005 *Physica A* **352** 131
[32] Zhang L Y and Wang P Y 2008 *Chin. Phys. Lett.* **25** 3818
[33] Narambuena C F, Beltramo D M and Leiva E P M 2007 *Macromolecules* **40** 7336
[34] Wang L, Liang H and Wu J 2010 *J. Chem. Phys.* **133** 044906
[35] Carrillo J M Y and Dobrynin A V 2007 *Langmuir* **23** 2472